Convective heat–mass transfer in the entrance region of a concentric annulus having a rotating inner cylinder

M. Molki*, K. N. Astill, and E. Leal
Department of Mechanical Engineering, Tufts University, Medford, MA, USA

Heat transfer characteristics of laminar flow in a circular annulus with a rotating inner cylinder in the presence of a laminar axial flow was investigated using sublimation techniques. The work focused on the entrance region of the annulus with simultaneous development of velocity and temperature profiles. The experiments were carried out using a mass transfer procedure. Measured mass transfer results were transformed to heat transfer quantities through the analogy between the two processes. The highest speed of rotation of the inner cylinder corresponded to a Taylor number of 500, which was sufficient to produce Taylor vortices in the flow. The axial flow Reynolds number, based on the hydraulic diameter, ranged from 500 to 1250. All experiments were carried out for the radius ratio $N=0.8$. The working fluid was air at room temperature and pressure. Results correspond to the case for heat transfer with an isothermal inner cylinder and an adiabatic outer cylinder.

Keywords: annular flow; convective heat–mass transfer; developing flow and heat transfer; rotating annular flow; Taylor vortex flow; sublimation techniques for heat transfer

Introduction

Annular geometries with heat transfer to axially flowing fluids are frequently encountered in engineering systems. The heat transfer problem often is complicated by having an annulus with a rotating inner cylinder and a stationary outer cylinder. This problem might be encountered, for example, in cooling of electrical machinery and bearing lubrication. When rotation rates exceed a certain value, a secondary flow occurs in the form of pairs of vortex rings or spirals—the so-called Taylor vortices. In annuli usually encountered in engineering problems, the axial length required for the development of velocity profiles, heat transfer, and the vortex system can be a significant fraction of the total length. To design such systems accurately, we must understand the behavior of the flow as the flow develops. Hence we conducted this investigation to determine heat and mass transfer characteristics in a circular annulus having a rotating inner cylinder with an axial flow. We limited the investigation to the entrance region, where the velocity and temperature or concentration profiles develop simultaneously.

Taylor[1] demonstrated analytically and experimentally the existence of a secondary vortex flow between concentric cylinders when the inner cylinder rotates and the outer cylinder is stationary. Kaye and Elgar[2] imposed an axial flow and observed four modes of flow: (1) laminar; (2) laminar with vortices; (3) turbulent; and (4) turbulent plus vortices. Since that time, other modes, such as spiral, wavy, etc., have been observed. Astill[3] examined the development of vortex flow in the entrance region of the concentric annulus when an axial flow was present.

Demarcation lines among the flow modes have been determined for various radius ratios in fully developed flow in terms of the flow parameters for both adiabatic and diabatic flow. Studies of heat transfer in this geometry have been restricted to a few special cases. Coney and El-Shaarawi[4] and Lundberg *et al.*[5,6] have analyzed the problem of heat transfer in an annulus with developing laminar flow without cylinder rotation. Both present results with an isothermal inner cylinder and an adiabatic outer cylinder. Three other wall boundary conditions are analyzed in ref. 7.

Experimental heat transfer results are given for fully developed flow with a rotating inner cylinder in Becker and Kaye.[8] Coney and El-Shaarawi[9] extended their finite difference analyses of the heat transfer in developing laminar flow to the case of inner-cylinder rotation. In their analysis, velocity and temperature profiles develop simultaneously with an isothermal inner wall and an adiabatic outer wall. Results are given for $N=0.85$, prior to the onset of Taylor vortices. Payne and Martin[10] used finite-difference techniques to solve the equations for developing laminar heat transfer in elliptic form. These models were based on a uniform heat flux from the rotating inner cylinder and an adiabatic outer cylinder with $N=0.9$. Axial velocity was assumed to be fully developed. Although the analysis was confined to flow without Taylor vortices, limited experimental results were given for the same conditions of flow and geometry in the annulus where Taylor vortices have occurred.

Experimental techniques that can be utilized in the combined thermal–hydraulic entry length problem include measuring temperature profiles in the annular gap or using a series of individually controlled heaters along the axis. Application of these techniques is difficult for a rotating boundary. Tests using resistance heating techniques experience thermal losses to the structure, producing experimental error. When wall heat flux or surface temperatures are predicted by extrapolating temperature gradients in the gap near the wall, small errors in measurement of temperatures can lead to large errors in the results.

In the present investigation, the resistance heating approach was replaced by the well-known naphthalene sublimation technique in an effort to increase the accuracy of the results

* Present address: Department of Mechanical Engineering, Esfahan University of Technology, Esfahan, Iran.
Address reprint requests to Professor Astill at the Department of Mechanical Engineering, Tufts University, Medford, MA 02155, USA.

Received 8 June 1989; accepted 3 November 1989

and to maintain better control over the boundary conditions.

In the heat transfer analog of the sublimation process, the outer wall becomes a perfect adiabatic wall, and conduction losses to the structure are eliminated. Furthermore, as the experiment is essentially isothermal, the mass transfer is analogous to a true isothermal inner wall for heat transfer experiments. The measured quantity was the rate of mass sublimated along the inner wall; subsequently, the analogy between heat and mass transfer processes was employed to transform the mass transfer results to heat transfer quantities. Because of this analogy, the terms mass transfer and heat transfer are used interchangeably throughout this article.

The major objectives of this effort were to determine the practicability of the naphthalene sublimation technique in this geometry and to obtain heat transfer data for laminar flows.

Experimental apparatus and procedure

The experimental apparatus and corresponding instruments are shown schematically in Figure 1. The heart of the apparatus was the naphthalene test section, where the mass transfer occurred. The test section—consisting of a plexiglass outer cylinder (6.350 + 0.004 cm ID) concentric with a naphthalene-coated inner cylinder (5.080 cm OD)—was an annular passage with a gap of 0.635 + 0.008 cm and a radius ratio of 0.8. The inner cylinder had a modular design that allowed the rate of mass transfer to be monitored at any given axial station along the annulus.

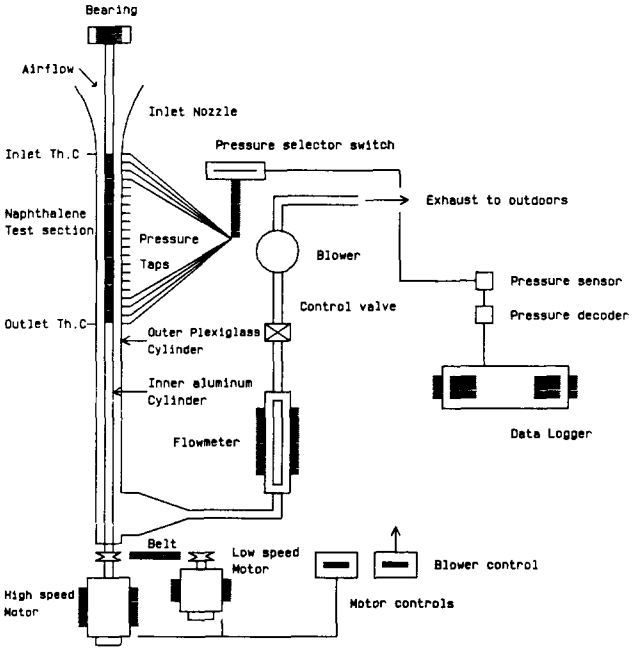

Figure 1 Schematic view of the experimental apparatus

The rotating portion of the inner cylinder began at the farthest upstream end of the test section and right at the point where the mass transfer species was introduced into the air stream. This arrangement was intended to eliminate any initial swirling motion of the air stream before it entered the annulus. Consequently, the velocity and concentration (temperature) profiles developed simultaneously.

Each module of the test section was a short hollow cylinder made of aluminum with inner and outer diameters of 2.54 cm and 4.45 cm, respectively. The outside cylindrical surface of the modules was knurled to facilitate the adhesion of solid naphthalene. When coated with solid naphthalene, the modules attained an outside diameter of 5.080 + 0.004 cm, which was equal to the diameter of the inner cylinder of the annulus.

Twenty modules of three different sizes were used. Each of the first four had an axial length of 0.635 cm; each of the next four, 1.27 cm; and each of the remaining twelve, 2.54 cm. The small modules were positioned along the farthest upstream portion of the naphthalene test section; the medium and large modules were placed in the middle and farther downstream, respectively. This arrangement provided more data points near the inlet, where variations of transfer coefficients are normally large. Moreover, the last module was intended to maintain the continuity of mass (thermal) boundary conditions in the neighborhood of the point where the naphthalene coating ended. Therefore no calculations were made using the data from this module.

A converging nozzle with an elliptic surface was installed at the upstream end of the annulus to control flow separation. This nozzle was fabricated by a casting and machining process, using plastic resin and catalyzers, which are the main ingredients of commercially available plexiglass. At the entrance to the test section, the boundary layer thickness of the axial velocity was about 14% of the gap at a Reynolds number of 700.

Two variable-speed electric motors were utilized to drive the inner cylinder assembly. As shown in Figure 1, the high-speed motor (a $\frac{1}{2}$HP variable-speed Minarik), which was equipped with a magnetic pick-up and RPM readout, was connected directly to the drive shaft. The low-speed motor ($\frac{1}{8}$HP) provided lower speeds of rotation. Motor speed was controlled by a variable-power supply unit that could vary the voltage from 0 to 140 V.

Notation

A_i	Mass transfer area per module
D_h	Hydraulic diameter, $2(r_2 - r_1)$
$\mathscr{D}$	Diffusion coefficient
h	Heat transfer coefficient
K_i	Mass transfer coefficient for module i
k	Thermal conductivity
M_i	Mass change for module i
N	Radius ratio, r_1/r_2
Nu	Nusselt number, hD_h/k
Pr	Prandtl number
Q	Volumetric air flow rate
Re	Reynolds number, VD_h/v
r_1, r_2	Inner and outer radii of the annulus
Sc	Schmidt number, $v/\mathscr{D}$
Sh_i	Per-module Sherwood number, $K_iD_h/\mathscr{D}$
Ta	Taylor number, $\Omega r_1 D_h/2v$
V	Mean axial velocity
X	Axial coordinate
z	Dimensionless axial coordinate, $X/(D_h\mathrm{ReSc})$

Greek symbols

v	Kinematic viscosity
Ω	Angular velocity of the inner cylinder
τ	Duration of data run
ρ_{nw}	Naphthalene vapor density at wall
$\rho_{nb,i}$	Naphthalene vapor density in bulk at module i

The annulus and the electric motors were all mounted on and secured to a 15.2-cm × 183.0-cm aluminum channel beam. After all components were assembled and aligned, the channel beam was bolted vertically to the laboratory wall.

A number of pressure taps were deployed along the test section. The first tap was selected as a reference, and the pressure at any other tap was measured with respect to it. Pressure signals were monitored with a Baratron pressure transducer with a resolution of 0.001 mm Hg and were recorded on a Fluke 2200B Datalogger.

The day before each data run, the naphthalene modules were prepared by a casting operation. To facilitate the casting, a four-component mold was fabricated from aluminum. A hollow cylinder, a solid shaft, and two end caps were the components of the mold. The shaft was positioned in the middle of, and concentric with, the hollow cylinder. Then one of the test section modules was mounted on the shaft to form an annular gap between the module and the cylinder. The two caps were subsequently used to close the openings at the two ends of the mold. Next, the assembled mold was filled with molten naphthalene through a pouring aperture. When the naphthalene had solidified, the mold was disassembled and the module, which now had a coating of solid naphthalene on the outside, was removed.

The casting procedure was repeated for each module. Then each module was wrapped in plastic to prevent sublimation. All modules remained in the laboratory overnight in order to attain thermal equilibrium.

Prior to a data run, the blowers, data logger, and electric motors were turned on to warm up the apparatus. At the same time, a computer program was activated on an Apple II computer to estimate the desired Reynolds–Taylor number combination with a trial-and-error procedure. Subsequently, each module was weighed on a Sartorious 2432 balance that could resolve up to 0.1 mg. The apparatus was then turned off and the modules were mounted on the inner cylinder and firmly secured. When the airflow was reactivated, the sublimation process began and the mass of each module changed. After 50 minutes, the apparatus was turned off again, and the modules were weighed for a second time. The difference between the two measurements provided the mass sublimation from the inner cylinder at various axial stations. Average mass-change values for all tests were 0.021 g for the smallest modules and 0.030 g for the largest. These values are equivalent to removal of naphthalene to a depth of 0.02 mm from the small modules and 0.007 mm from the large modules—a change of diameters of 0.08% and 0.02%, respectively. Consequently, it was possible to make a second run with the same modules without significant changes in diameter.

Also recorded during the run were the naphthalene surface temperature, barometric pressure, air pressure inside the test section, volumetric flow rate, and RPM of the inner cylinder. Air temperatures were measured with a copper–constantan thermocouple, located 0.2 cm from the naphthalene surface at the entrance and exit of the test section. On average, the maximum temperature variation along the naphthalene surface was about 0.1°C.

Mass (heat) transfer results

The mass transfer coefficients reported here are nondimensional and are presented in terms of Sherwood number:

$$\mathrm{Sh}_i = \frac{K_i D_h}{\mathscr{D}} \tag{1}$$

Because the transfer coefficients vary along the test section, the subscript i is used to denote quantities related to the ith module. In Equation 1, the diffusion coefficient for sublimation of naphthalene into air is obtained from the expression

$$\mathscr{D} = \frac{\nu}{\mathrm{Sc}} \tag{2}$$

with Schmidt number Sc = 2.5 (see ref. 11).

Dimensional mass transfer coefficients K_i were determined from the conventional definition

$$\Delta\rho_i = \frac{M_i/A_i}{\Delta\rho_{n,i}} \tag{3}$$

where $\Delta\rho_{n,i} = \rho_{nw} - \rho_{nb,i}$ is the wall- to bulk-naphthalene vapor-density difference. The density of naphthalene vapors at the wall were evaluated from the ideal gas equation in conjunction with the equation for vapor pressures reported by Sogin.[11]

The calculation of the bulk density of naphthalene $\rho_{nb,i}$ for airflow at axial station i was carried out by performing a mass balance over a portion of the test section. Laboratory air free from naphthalene vapors means that $\rho_{nb} = 0$ at the inlet, which yields

$$\rho_{nb,i} = \sum_{j=1}^{i} \left(\frac{Mj}{\tau}\right) Q \tag{4}$$

Since the pressure drop along the annular duct was small, the effect of pressure variations on the volumetric flow rate Q was negligible.

In our results, Reynolds and Taylor numbers appear as parameters with the definitions

$$\mathrm{Re} = \frac{V D_h}{\nu} \tag{5}$$

$$\mathrm{Ta} = \frac{\Omega r_1 D_h}{2\nu} \tag{6}$$

In Equations 5 and 6, V and Ω are the mean velocity of air in the annulus and the angular velocity of the rotating inner cylinder, respectively. The kinematic viscosity ν that appears in Equations 2, 5, and 6 is evaluated for pure air with the assumption that the amount of naphthalene vapor present in air has a negligible effect on kinematic viscosity.

The mass transfer coefficients for the case of no rotation (Ta = 0)—and evaluated from Equation 1—are presented in Figure 2. The Reynolds number appears as a parameter. The abscissa, X/D_h, indicates the normalized axial distance from the inlet, with $X = 0$ corresponding to the upstream end of the annulus where the naphthalene coating begins.

The Sherwood numbers are very large close to the inlet. Downstream, the Sherwood number decreases exponentially, approaching the value for fully developed flow. This result is to be expected, as the concentration gradient of the subliming species is larger in the vicinity of the inlet, resulting in larger coefficients. However, as the boundary layer grows along the flow, the concentration gradients diminish and the Sherwood numbers decrease.

An increase in the Reynolds number has a retarding effect on the growth of the boundary layer, which, in turn, enhances mass (heat) transfer at any location. This trend is demonstrated in Figure 2, where an increasing Re has the effect of increasing the Sherwood number in the developing flow. The fully developed value of the Sherwood number is independent of the Reynolds number and is approximately 5.2.

Figures 3 and 4 show the effect imposed by the rotating inner wall on the transfer coefficients. Rotation of the inner wall produced two effects on the rate of mass transfer. The more obvious effect is a rapid increase in mass transfer at $X/D_h = 16$, which occurs for all Reynolds numbers tested at the largest

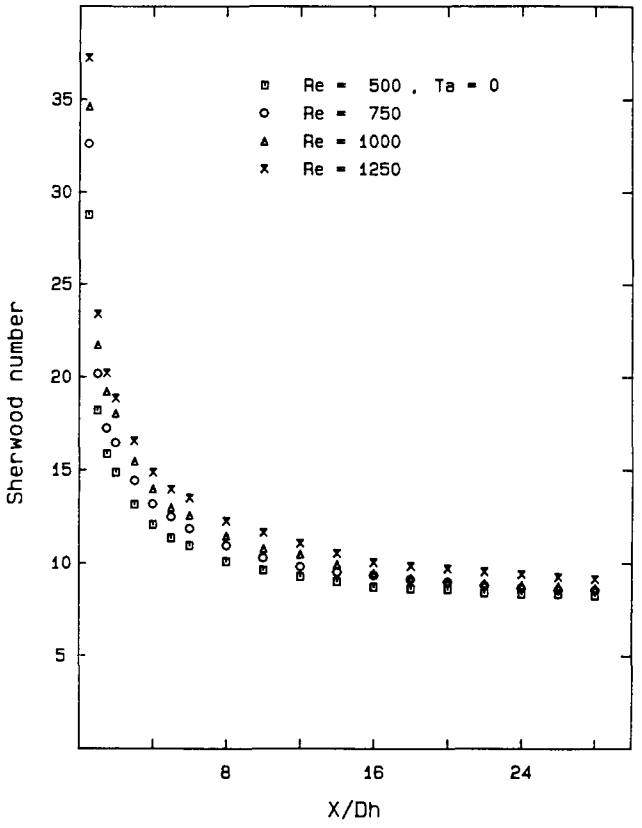

Figure 2 Distribution of Sherwood number for Ta = 0

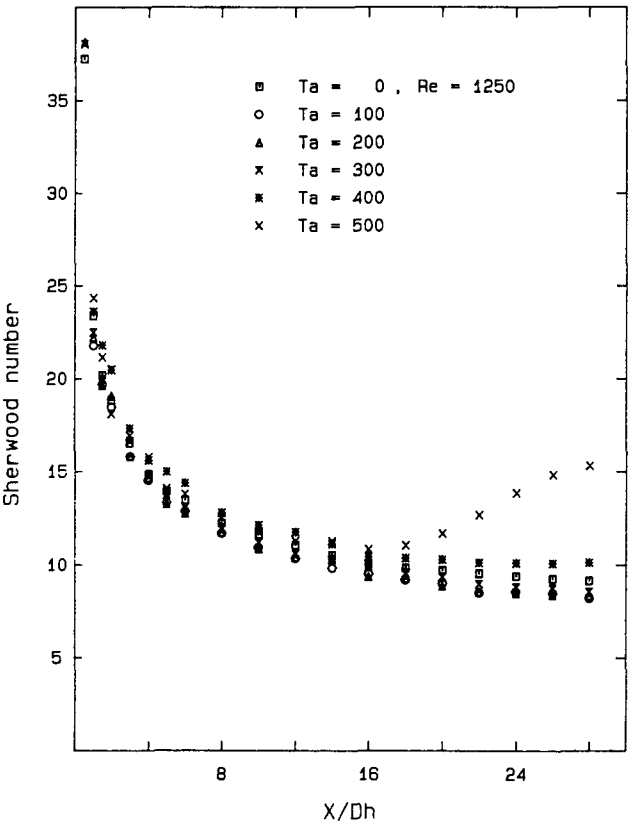

Figure 4 Effect of rotation on Sherwood number, Re = 1250

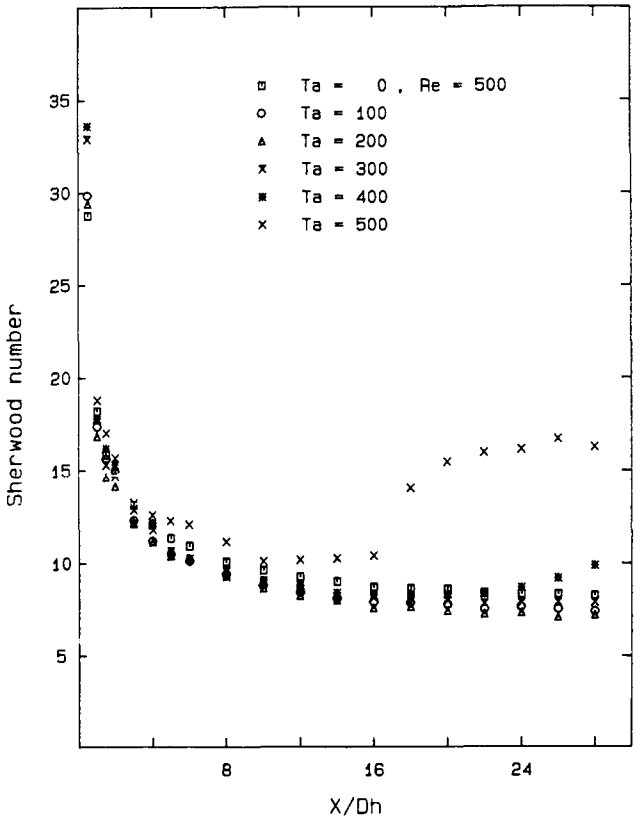

Figure 3 Effect of rotation on Sherwood number, Re = 500

Taylor number, 500. The increase is apparent for the two cases shown in Figures 3 and 4, in which the Reynolds numbers are 500 and 1250, respectively. It is also obvious at a Taylor number of 400 at $X/D_h \simeq 24$, when the Reynolds number is 500. This condition probably occurred at the onset of the Taylor vortices in the developing flow. The rapid increase in Sherwood number behaved in the expected manner, moving toward the entrance as the Taylor number was increased and away from the entrance for increasing Reynolds numbers, as observed by Astill.[3]

We evaluated this assumption by introducing smoke into the annulus, in which we had replaced the naphthalene inner cylinder with an aluminum cylinder of the same diameter. The radial plane was illuminated by passing light from a laser source through a glass rod with its axis normal to the axis of rotation of the annulus. A discernible oscillation occurred in the smoke trace at the start of the Taylor vortex system. This system is followed in the flow by development of the vortices downstream. The flow was entirely laminar in these tests. The distance to the first discernible oscillation was measured from stopped frames of video tape. Transition points determined in this way for four Reynolds numbers and a Taylor number of 500 are shown on the mass transfer curves of Figure 5. Transition points from the smoke tests are all slightly upstream from the point where the mass transfer curves show an increase. For the four cases for which smoke tests were run, the values of X/D_h at transition for a Taylor number of 500 were Re = 500, $X/D_h = 7$; Re = 750, $X/D_h = 10$; Re = 1000, $X/D_h = 12$; and Re = 1250, $X/D_h = 15$. We can reasonably conclude that the upturn in mass transfer is caused by the transition to vortex flow and that it is not experimentally significant until the vortices become established after the first discernible oscillations have occurred.

The second effect occurred at low Taylor numbers prior to the onset of Taylor vortices. As the Taylor number was increased to a value of 200, the Sherwood number was lower

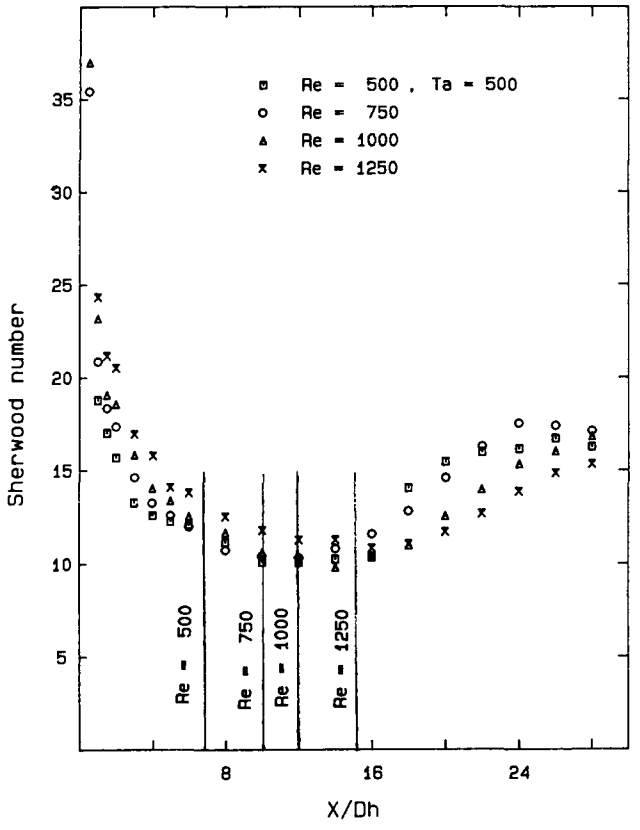

Figure 5 Effect of Reynolds number for Ta = 500, showing observed points of transition to vortex flow

than for Ta = 0. This result was most apparent at the low Reynolds number flow. At a Reynolds number of 500 it did not reach the values found for no rotation until the Taylor number reached 400. This characteristic, which diminished for the higher Reynolds number flows, was observed in fully developed flow by Wan and Coney,[12] who did not offer an explanation. Although we could argue that the range of values is within the expected range of error, the consistency and reproducibility of these results begs a comment. We hypothesize that the effect of the circulation on the tangential boundary layer may cause the denser naphthalene to move radially outward, thus flattening the distribution of the concentration gradients. It is noteworthy that Wan and Coney used a heated outer cylinder, which would also place the denser air near the inner cylinder in the tangential boundary layer.

In the entrance region of the annulus where the hydrodynamic and mass concentration boundary layers grow simultaneously, the Schmidt number and Reynolds number play important roles and determine the relative growth of the two boundary layers. This argument led us to define an axial parameter $z = X/(D_h \mathrm{ReSc})$, which incorporates the Reynolds and Schmidt numbers into the length parameter. We included the Schmidt number to ensure consistency with the heat transfer results of investigators who had employed a length parameter of $X/(D_h \mathrm{RePr})$.

Correlation of results

The mass transfer results corresponding to Ta = 0 were brought together through the preceding definition of z and are presented in Figure 6. Data for all Reynolds numbers are shown. The least squares procedure fit the experimental data with the equation

$$\mathrm{Sh} = 5.21 + 0.48 z^{-0.451} \tag{7}$$

which is represented by the solid line in Figure 6. The constant term in Equation 7, 5.21, represents the fully developed value for the Sherwood number. It was based on an average of values for all data using a best-fit criterion. The data included cases with rotation of the inner cylinder prior to vortex formation, with the range of values going from 5.06 to 5.37. The value of the mean, 5.21, agreed well with the fully developed Nusselt number of 5.25 interpolated for $N = 0.8$ from ref. 7 for the case of an isothermal inner surface and adiabatic outer surface. Because the Schmidt number here is a fixed value, we can eliminate it from the parameter z by changing the constant from 0.48 to 0.73.

Several investigators have dealt with the problem of convective heat transfer in an annulus having a developing laminar flow but with no rotation of the inner cylinder. To compare results, we had to convert the mass transfer results to heat transfer parameters, using the well-known analogy between heat and mass transfer. This conversion entails determining how the Prandtl and Schmidt numbers enter the process. Expressing the Sherwood and Nusselt numbers as

$$\mathrm{Sh} = Cf(\mathrm{Re})\mathrm{Sc}^n \quad \text{and} \quad \mathrm{Nu} = Cf(\mathrm{Re})\mathrm{Pr}^n$$

and assuming that the functional behavior with the Reynolds number and the constant C are the same, we deduce that

$$\mathrm{Nu} = \mathrm{Sh}\left(\frac{\mathrm{Pr}}{\mathrm{Sc}}\right)^n \tag{8}$$

Typical values for the exponent n are 0.4 or $\frac{1}{3}$ for laminar flow. Based on a comparison of the present results to those in ref. 7, we selected a value of $n = \frac{1}{3}$ for the analogy. However, we

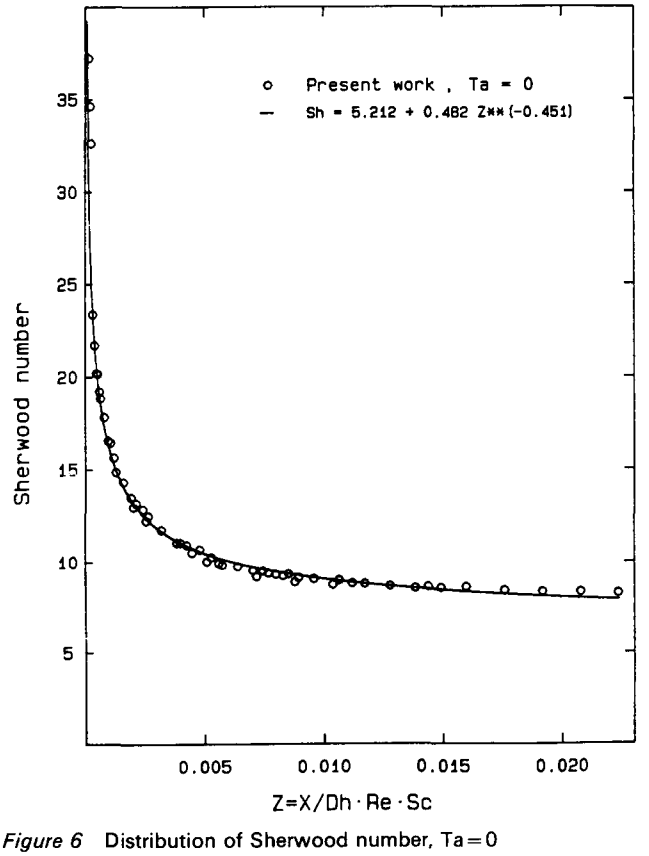

Figure 6 Distribution of Sherwood number, Ta = 0

cannot guarantee that this is the most appropriate value solely on the work reported here. For a Schmidt number of 2.5 and a Prandtl number of 0.7, the relation becomes

$$\mathrm{Nu}=0.654\mathrm{Sh} \tag{9}$$

Using the heat transfer length parameter of ref. 5, $X/(D_h\mathrm{Re}\,\mathrm{Pr})$, the conversion from z is

$$\frac{X}{(D_h\mathrm{Re}\,\mathrm{Pr})}=3.571z \tag{10}$$

Figures 7, 8, and 9 compare our results and those of several other investigators for heat transfer in stationary annuli. Lundberg *et al.*[6] analyzed the general problem of convective heat transfer in a stationary annulus with a fully developed hydrodynamic flow and developing thermal boundary layers. In Figure 7, we compare their results for an isothermal inner wall and adiabatic outer wall for three radius ratios to our results. Our results for $N=0.8$ are slightly higher than those obtained by Lundberg *et al.* for $N=0.5$, near the entrance. Their asymptotic values of Nusselt number are 7.37 for $N=0.25$, 5.79 for $N=0.50$, and 4.90 for $N=1.00$. For our test results at $N=0.80$, the fully developed Nusselt number, or asymptotic value, is 5.21.

Using a finite-difference procedure, Coney and El-Shaarawi[4] studied heat transfer in a stationary annulus with the same wall conditions we used. Their analysis also used simultaneously developing thermal and hydrodynamic boundary layers, with flat profiles at the inlet. Our data for $N=0.8$ had slightly higher Nusselt numbers than did their values for $N=0.5$, with larger discrepancies for $N=0.9$.

Comparing the values from ref. 4 and those of ref. 6, the agreement is good for $N=0.5$ and $N=0.25$ (not shown here). However, comparing Nusselt numbers at $N=0.9$ from ref. 4

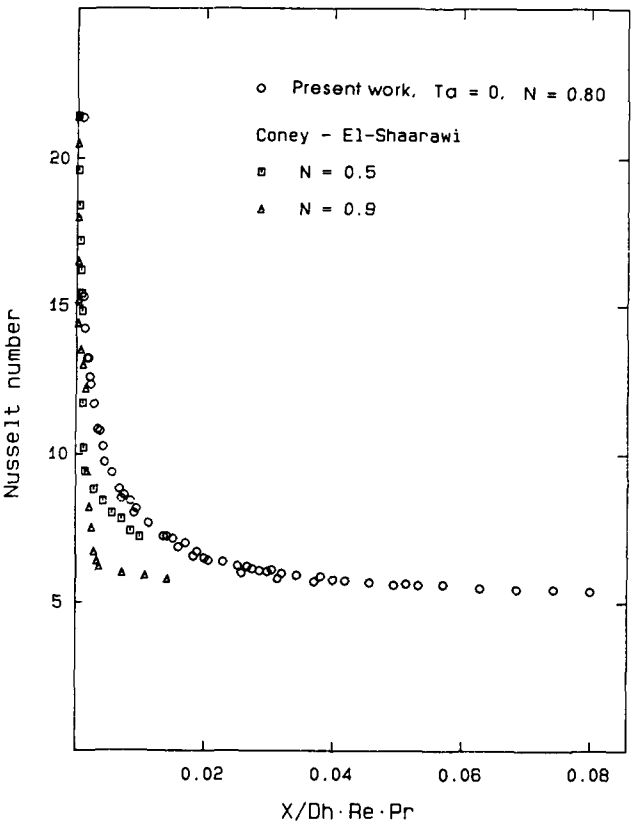

Figure 8 Comparison with the literature, Ta = 0

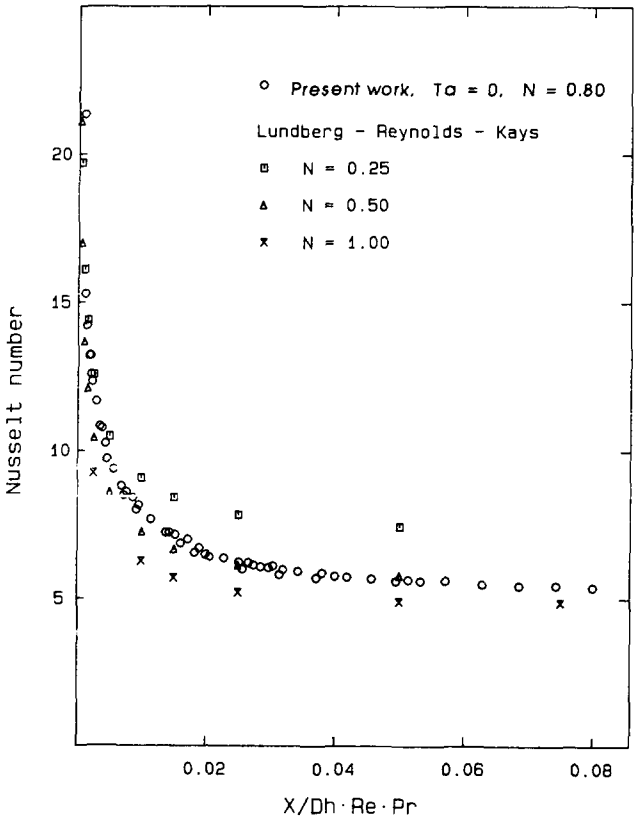

Figure 7 Comparison with the literature, Ta = 0

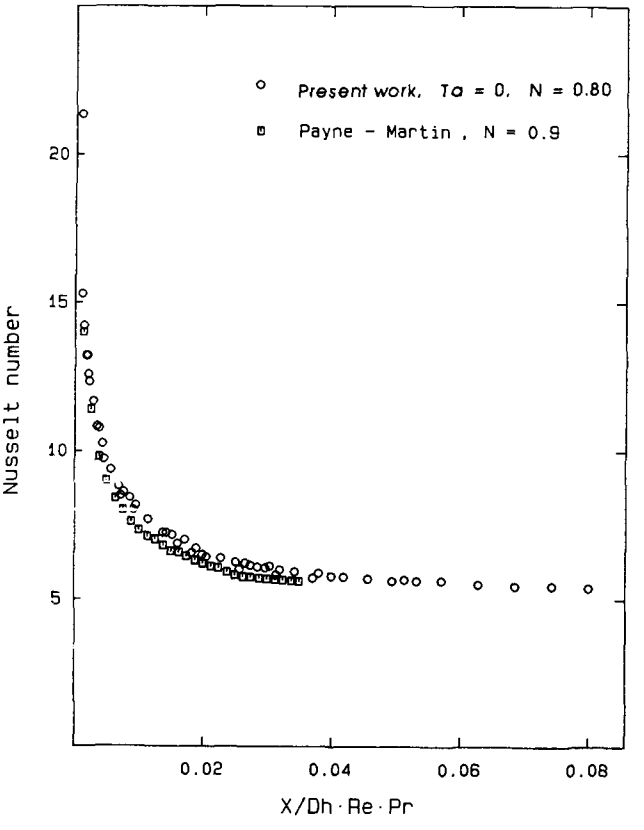

Figure 9 Comparison with the literature, Ta = 0

to those at $N = 1.0$ from ref. 6, shows that the Nusselt numbers in ref. 4 are smaller for length parameters less than 0.02. This result is contrary to what we would expect. These differences may be caused by the direct conversion of the length parameter used by Coney and El-Shaarawi to that used by us and by Lundberg *et al.*. The differences are particularly sensitive to the radius ratio, especially at the larger values of N.

Payne and Martin[10] used a finite-difference procedure to predict laminar heat transfer with uniform heat flux from the inner rotating core of a concentric annulus to the axially flowing fluid in the absence of vortex flow when the outer surface was adiabatic. Although the boundary conditions are different from those of our investigation, the two problems are expected to have a similar qualitative behavior. Higher heat transfer coefficients are usually observed at uniform heat flux rather than at uniform temperature from the inner cylinder. However, when the radius ratio N of the inner to outer cylinder is increased, the transfer coefficients are decreased. Because of these two opposing factors, the two sets of results shown in Figure 9 are surprisingly close. Moreover, considering the different thermal and hydrodynamic conditions of our investigation and those in literature, better agreement between results could not be expected.

Flow with cylinder rotation

The mass transfer data for flow with cylinder rotation for $Ta = 100$, 200, and 300 showed little deviation from those with no rotation. In each case, the Taylor number was not high enough for vortices to develop in the test section. These results, shown in Figures 10, 11, and 12, correlated so well in terms of the parameter z, that there is no distinction among the several Reynolds numbers. Consequently, no distinction is made among

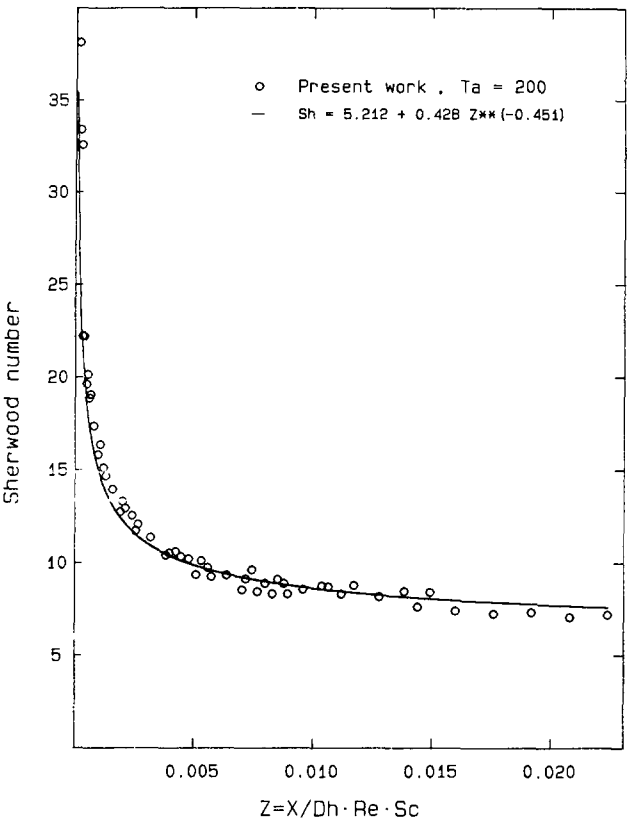

Figure 11 Distribution of Sherwood number, $Ta = 200$

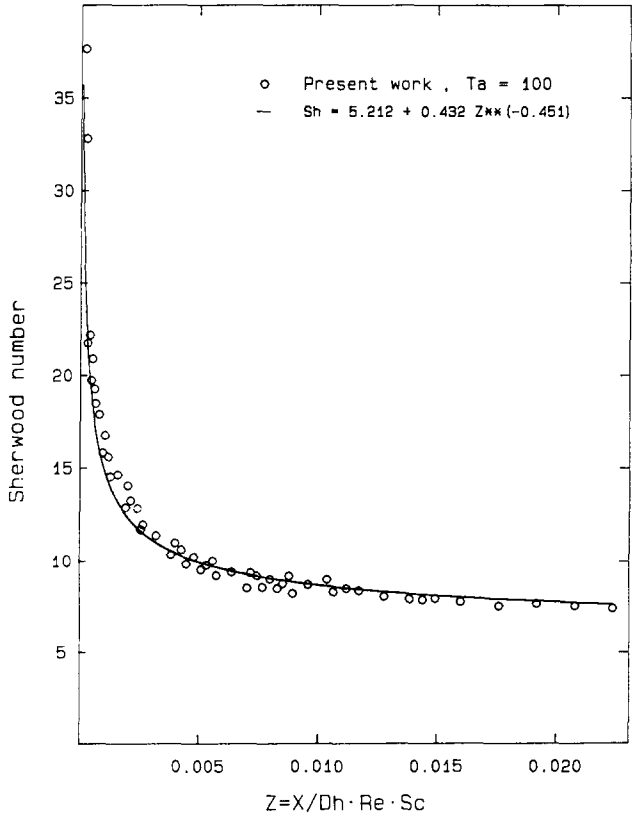

Figure 10 Distribution of Sherwood number, $Ta = 100$

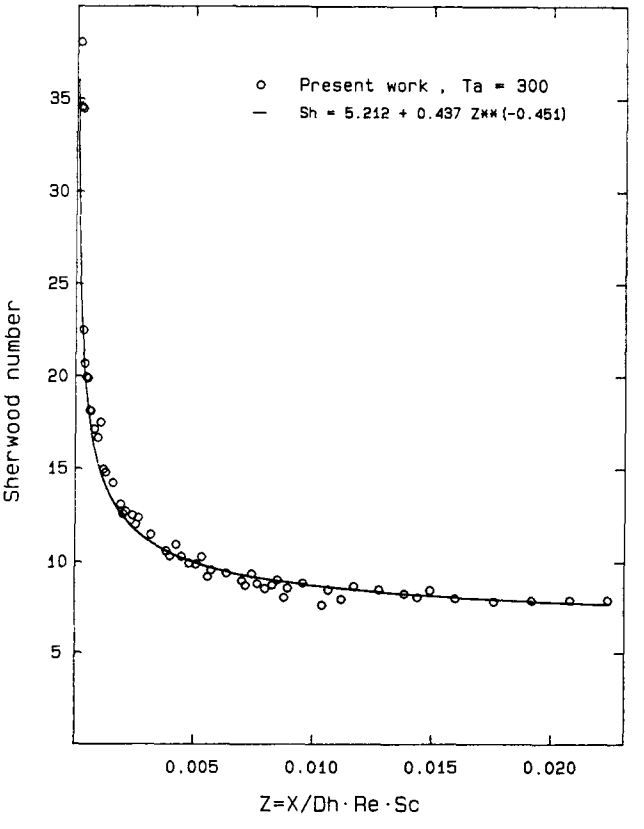

Figure 12 Distribution of Sherwood number, $Ta = 300$

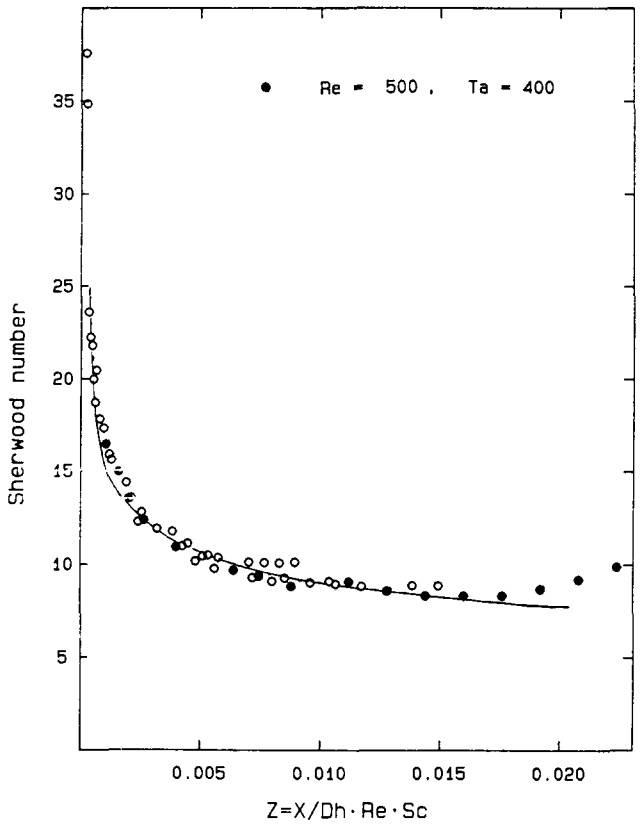

Figure 13 Distribution of Sherwood number, Ta = 400

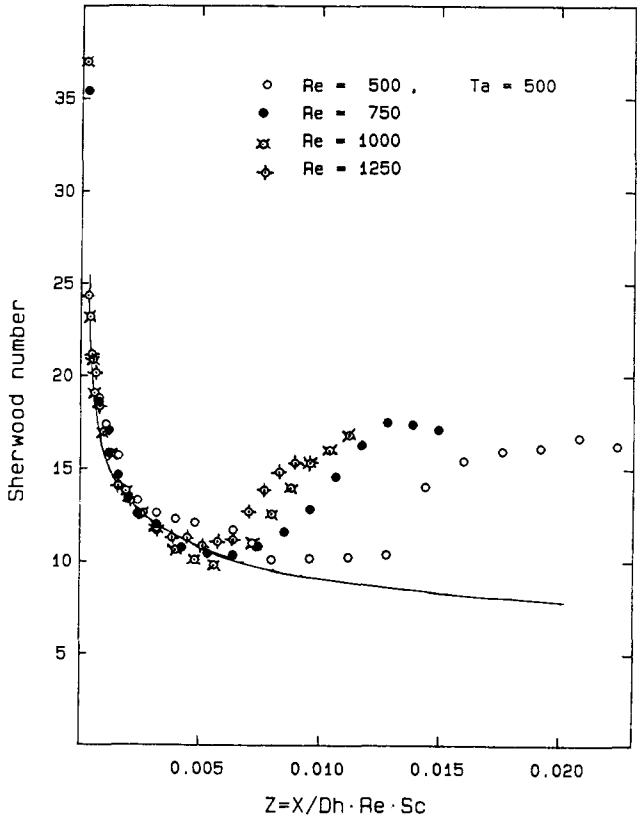

Figure 14 Distribution of Sherwood number, Ta = 500

the data points on the graphs. Although the boundary layer is not purely axial, as for the case with no rotation, the mass transfer in stable flow is similar enough to be fit by a curve having the same form as that given by Equation 7.

Moreover, examination of the momentum and energy equations for the axisymmetric laminar flow reveals some interesting facts about the fully developed flow. The momentum equations become uncoupled so that the axial velocity and tangential velocity are independent. In other words, rotation does not influence the axial profile, and the axial flow rate does not affect the tangential component. When the energy equation is considered, the conditions of axial symmetry and fully developed flow leads to the conclusion that heat (or mass) transfer is independent of the tangential component of velocity. Therefore the fully developed Nusselt (or Sherwood) number at speeds of rotation below those causing Taylor vortices, approaches the same asymptotic value as that for the case of no rotation. Consequently, the constant in the equations representing the stable flow with rotation were set as 5.21.

These arguments do not hold for developing flow. For the three sets of data, the coefficients, found by fitting each by the method of least squares, were slightly different: Ta = 0, 0.482; Ta = 100, 0.432; Ta = 200, 0.428; and Ta = 300, 0.437. Exponents were found to be 0.45. As noted earlier, the transfer rate was reduced slightly when rotation was imposed. As hypothesized earlier, this may be due to a reduction in the concentration gradient due to tangential flow. If the coefficient is taken as the mean, 0.445, the maximum difference among the coefficients and this value is 8.3%. This approach leads to errors in Sherwood number of less than 8% for all data. As the maximum deviation among the data from curve fitting was 8%, the argument that the variation was physical is invalid. In their finite-difference analysis, Coney and El-Shaarawi[9] show that an increase in Taylor number causes a slight increase in Nusselt number for a given Reynolds number. For a change from zero rotation (Re^2/Ta)† of 0 to a value of $(Re^2/Ta)^* = 1$, the increase went from 0% to 2%. Consequently, we recommend an average value for the coefficient of 0.445, making the general form of the relation

$$Sh = 5.21 + 0.445z^{-0.451} \tag{11}$$

applicable to Taylor numbers from 0 to 300. In the region of stable flow for a Taylor number of 300, the results given in ref. 9 require our Reynolds number to be 900. Using results for all Reynolds numbers and a Taylor number of 300, we found that present data converted to Nusselt numbers by analogy were slightly larger than the results of Coney and El-Shaarawi.[9] Using Equation 11, we found that the differences between the calculated values of Nusselt numbers and those of ref. 9 varied from 15% at $z = 0.001$ to 0% at $z = 0.02$.

When the Taylor number was increased to 400 and 500, vortices developed in the test section. They occurred for all Reynolds numbers at Ta = 500 and at a Reynolds number of 500 for Ta = 400. Results are shown in Figures 13 and 14, with data identified for each Reynolds number. Imposed on the graphs is the curve representing Equation 11. It appears to fit the data well in the stable region at Ta = 400 and to give slightly smaller values of Sherwood number than the stable test data at Ta = 500.

Conclusions

Our investigation seemingly is the first time that the naphthalene sublimation technique has been applied to an annulus with a

† The expression $(Re^2/Ta)^*$ refers to definitions of Taylor and Reynolds numbers in ref. 9. For the radius ratio, N = .8, it is related to our definition as $Re^2/Ta^2 = (Re^2/Ta)^*$ (0.11).

rotating inner cylinder in order to study heat transfer in the entrance region. The analogy between heat and mass transfer processes enabled us to compare the present mass transfer results with heat transfer data. The good agreement achieved supports the mass transfer technique. Consistency within the data was most encouraging.

We showed that, when the flow is stable, the mass transfer results can be correlated by using a parameter $z = X/D_h \mathrm{ReSc}$. Data can be represented by the relation

$$\mathrm{Sh} = 5.21 + 0.45 z^{-0.45}$$

for Taylor numbers as high as 400.

At high rotation speeds, a transition to vortex flow occurred, and the mass transfer coefficients were enhanced. The fully developed Sherwood number, found to be 5.21 for stable flow, increased to 15 or 16, depending on the value of the Taylor number, when vortices occurred. Further, the axial location of the transition was related to the flow Reynolds number. As the Reynolds number was increased, the vortices moved farther downstream, and as the speed of rotation increased, the transition point moved upstream.

The behavior and location of this transition is consistent with visual studies. Using a smoke tracer in the apparatus, we observed that the transition points were located slightly upstream of the point where an increase in the mass transfer rate occurred.

References

1 Taylor, G. I. Stability of a viscous fluid contained between two rotating cylinders. *Phil. Trans. A.*, 1923, **223**, 289–343

2 Kaye, J. and Elgar, E. C. Modes of adiabatic and diabatic flow in an annulus with a rotating inner cylinder. *Trans. ASME*, 1958, **80**, 753–765

3 Astill, K. N. Studies of the developing flow between concentric cylinders with the inner cylinder rotating. *ASME J. of Heat Transfer*, 1964, **86**, 383–392

4 Coney, J. E. R. and El-Shaarawi, M. A. I. Laminar flow heat transfer in concentric annuli with simultaneously hydrodynamic and thermal boundary layers. *Int. J. Num. Meth. Eng.*, 1975, **9**, 17–38

5 Lundberg, R. E., Reynolds, W. C., and Kays, W. N. Heat transfer with laminar flow in concentric annuli with constant and variable wall temperatures with heat flux. NASA Tech. Note D1972, 1963

6 Lundberg, R. E., McCuen, P. A., and Reynolds, W. C. Heat transfer in annular passages: Hydrodynamically developed laminar flow with arbitrarily prescribed wall temperatures on heat fluxes. *Int. J. Heat Mass Transfer*, 1963, **6**, 495–529

7 Heaton, H. S., Reynolds, W. C., and Kays, W. M. Heat transfer in annular passages: Simultaneous development of velocity and temperature fields in laminar flow. *Int. J. Heat Mass Transfer*, 1964, **7**, 763–781

8 Becker, K. M. and Kaye, J. Measurements of diabatic flow in an annulus with an inner rotating cylinder. *ASME J. of Heat Transfer*, 1962, **82**, 97–105

9 Coney, J. and El-Shaarawi, M. A. I. Laminar heat transfer in the entrance region of concentric annuli with rotating inner walls. *ASME J. of Heat Transfer*, 1974, **96**, 560–562

10 Payne, A. and Martin, B. W. Heat transfer in laminar flow in a concentric annulus from a rotating inner cylinder. *Proc. 5th Int. Heat Transfer Conference*, Tokyo, 1974, 80–84

11 Sogin, H. H. Sublimation from disks to air streams flowing normal to their surface. *Trans. ASME*, 1958, **80**, 61–69

12 Wan, C. C. and Coney, J. E. R. An experimental study of diabatic spiral flow. *Int. J. Heat and Fluid Flow*, 1982, **3**, 31–38